# Mechanisms of Ephrin Receptor Protein Kinase-Independent Signaling in Amphid Axon Guidance in *Caenorhabditis elegans*

**Emily N. Grossman, Claudiu A. Giurumescu, and Andrew D. Chisholm[1]**
Division of Biological Sciences, Section of Cell and Developmental Biology, University of California, San Diego, La Jolla, California 92093

**ABSTRACT** Eph receptors and their ephrin ligands are key conserved regulators of axon guidance and can function in a variety of signaling modes. Here we analyze the genetic and cellular requirements for Eph signaling in a *Caenorhabditis elegans* axon guidance choice point, the ventral guidance of axons in the amphid commissure. The *C. elegans* Eph receptor EFN-1 has both kinase-dependent and kinase-independent roles in amphid ventral guidance. Of the four *C. elegans* ephrins, we find that only EFN-1 has a major role in amphid axon ventral guidance, and signals in both a receptor kinase-dependent and kinase-independent manner. Analysis of EFN-1 and EFN-1 expression and tissue-specific requirements is consistent with a model in which VAB-1 acts in amphid neurons, interacting with EFN-1 expressed on surrounding cells. Unexpectedly, left-hand neurons are more strongly affected than right-hand neurons by loss of Eph signaling, indicating a previously undetected left–right asymmetry in the requirement for Eph signaling. By screening candidate genes involved in Eph signaling, we find that the Eph kinase-independent pathway involves the ABL-1 nonreceptor tyrosine kinase and possibly the phosphatidylinositol 3-kinase pathway. Overexpression of ABL-1 is sufficient to rescue *EFN-1* ventral guidance defects cell autonomously. Our results reveal new aspects of Eph signaling in a single axon guidance decision *in vivo*.

EPHRINS and their cell surface receptors, the Eph receptor tyrosine kinases (EphR), play critical roles in many axon guidance processes, including midline guidance and growth cone collapse (Drescher *et al.* 1995; Cowan *et al.* 2000). In contrast to long-range guidance cues, Eph signaling involves short-range interactions between a transmembrane receptor and transmembrane (ephrin-B) or GPI-linked (ephrin-A) ligands. Eph signaling is complex and multifunctional, capable of mediating both repulsion and attraction depending on ephrin concentration even in the same neurons (Hansen *et al.* 2004). Many of the signaling pathways downstream of Eph receptors and ephrins regulate cell movement or cell adhesion (Kullander and Klein 2002; Pasquale 2005).

Because Eph receptors and ephrins are cell surface molecules, they can operate in a variety of signaling modes (Kullander and Klein 2002; Egea and Klein 2007; Pasquale 2008). Eph receptors can generate kinase-dependent "forward" signals, in which ligand binding triggers receptor dimerization, activating the intrinsic kinase activity of the receptor, and initiating responses in the receptor-expressing cell. Kinase-dependent forward Eph signaling contributes to many processes including retinotopic mapping (Hindges *et al.* 2002), axonal midline avoidance after crossing (Yokoyama *et al.* 2001), neural crest cell migration (Smith *et al.* 1997), and migration of neural progenitors (Catchpole and Henkemeyer 2011). This regulation of diverse developmental processes occurs in part via kinase-dependent interactions with downstream effectors including Src-family kinases (Zisch *et al.* 1998; Knoll and Drescher 2004), Rho GTPases (Wahl *et al.* 2000; Noren and Pasquale 2004), and RhoGEFs (Shamah *et al.* 2001; Sahin *et al.* 2005).

In addition to kinase-dependent signaling, some Eph receptors initiate kinase-independent forward signals. In HEK293 cells, EphA8 signals promote integrin activity via the phosphatidylinositol 3-kinase (PI3K) pathway; the juxtamembrane domain of EphA8 directly interacts with the PI3K catalytic subunit p110γ, independent of EphA8


doi: 10.1534/genetics.113.154393
Manuscript received June 17, 2013; accepted for publication August 16, 2013
Supporting information is available online at http://www.genetics.org/lookup/suppl/doi:10.1534/genetics.113.154393/-/DC1.
[1]Corresponding author: Division of Biological Sciences, 2402 Bonner Hall, 9500 Gilman Drive, MC 0368, La Jolla, CA 92093-0368. E-mail: chisholm@ucsd.edu

kinase activity (Gu and Park 2001, 2003). EphA8 can also interact with the Anks (ankyrin and sterile alpha motif) proteins AIDA and Odin in a kinase-independent manner (Shin *et al.* 2007). However, the significance of kinase-independent forward signaling *in vivo* has not been extensively analyzed. Reverse signaling via ephrin ligands can also contribute to kinase-independent functions. Although both ephrin-B and ephrin-A ligands are capable of reverse signaling (Bruckner *et al.* 1999; Davy *et al.* 1999), ephrin-A ligands do not contain a transmembrane domain and therefore require a coreceptor, such as p75 (Lim *et al.* 2008), TrkB (Marler *et al.* 2008), or Ret (Bonanomi *et al.* 2012).

In contrast to the many Eph receptors and ligands in vertebrates, *C. elegans* encodes a single Eph receptor, VAB-1 (George *et al.* 1998) and four ephrins, EFN-1–4 (Chin-Sang *et al.* 1999; Wang *et al.* 1999). The *C. elegans* ligands resemble vertebrate ephrin-As in topology, in that they are attached to the cell membrane by a glycosylphosphatidylinositol (GPI) linker. Ephrins EFN-1–3 have partly redundant roles in VAB-1 signaling, depending on the developmental context (Chin-Sang *et al.* 1999; Wang *et al.* 1999), whereas the divergent ephrin EFN-4 functions independently of VAB-1 (Chin-Sang *et al.* 2002; Ikegami *et al.* 2004).

*C. elegans* Eph signaling acts in diverse cell types and processes. VAB-1 and its ephrin ligands control neuroblast migrations during embryonic morphogenesis (George *et al.* 1998; Chin-Sang *et al.* 1999; Wang *et al.* 1999). The VAB-1 function in embryonic neuroblast migration requires both kinase-dependent and kinase-independent signaling, and involves partly redundant signaling by all three ephrin ligands. VAB-1 signaling also regulates oocyte maturation and gonadal sheath cell contractions in response to a distinct type of ligand, the major sperm proteins (Miller *et al.* 2003; Cheng *et al.* 2008). Although the VAB-1 kinase domain is required for inhibition of oocyte maturation in the absence of sperm, it is dispensable for regulation of the basal gonadal sheath cell contraction rate (Miller *et al.* 2003). *C. elegans* Eph signaling has been implicated in outgrowth or guidance of several axon types, including PLM outgrowth (Mohamed and Chin-Sang 2006) and pathfinding of PVQ and HSN axons (Boulin *et al.* 2006). In most of these situations, the defects of VAB-1/Eph receptor null mutants are more severe than those of kinase-dead alleles (George *et al.* 1998; Boulin *et al.* 2006; Mohamed and Chin-Sang 2006), implying that some VAB-1 signaling is kinase independent. However, the *in vivo* mechanism of VAB-1 kinase-independent signaling has remained elusive.

To understand the basis of VAB-1 kinase-independent signaling at the level of individual cells, we have focused on a simple axon guidance decision, the ventral guidance of amphid sensory axons. Ventral guidance of amphid sensory axons has been shown to require VAB-1 and at least two other partly redundant guidance pathways: netrin (UNC-6/UNC-40) signaling, and the SAX-3/Robo receptor (Zallen *et al.* 1999). Loss of function in any one of these pathways leads to incompletely penetrant guidance defects in which the amphid commissure extends laterally instead of ventrally. In these mutants the aberrant lateral axons extend anteriorly and enter the nerve ring, indicating that it is specifically the initial ventral guidance of amphid axons that is disrupted. Moreover, double mutants between the *vab-1*, *unc-40*, and *sax-3* pathways display strong synergistic enhancement of guidance defects, consistent with partial genetic redundancy. However as VAB-1 is also required for many aspects of embryonic morphogenesis, it has been unresolved whether VAB-1 acts directly in amphid axon guidance.

We show here that VAB-1 can function in amphid neurons to mediate their ventral axonal guidance, interacting with EFN-1 in nonamphid neurons. The requirement for Eph signaling displays an unexpected left–right asymmetry. VAB-1's role in amphid axon guidance involves at least two pathways, both of which are partly kinase independent. PI3K signaling promotes amphid axon guidance, acting at least partly in parallel to VAB-1; an additional role downstream of VAB-1 cannot be excluded. Additionally, ABL-1, a nonreceptor tyrosine kinase, signals in the amphid neurons as part of a VAB-1 kinase-independent pathway. These results elucidate mechanisms of VAB-1 kinase-independent forward signaling in amphid axon guidance.

## Materials and Methods

### *Strains and culture conditions*

Worms were cultured on *Escherichia coli* OP50 seeded NGM agar plates. Animals were grown and analyzed at room temperature (21–23°) with the exception of *pdk-1(sa709)* strains, which were analyzed at 22.5°, and *age-1(hx546)* and *aap-1(m889)*, which were analyzed at 25°. The following mutants were used: LGI: *unc-40(e1430)*; *aap-1(m889)*; *shc-1(ok198)*; *src-1(cj293)*, *src-2(ok819)*, *vpr-1(tm1411)*, *daf-16(mu86)*, and *goa-1(sa734)*; LGII: *vab-1(ju8*, *e2027*, *ju307*, *ok1699*, *dx14*, *dx31*, *ju220*, *ju275*, *e858*, *e699*, *ju306*, *tn2*, *e118*, *zd118*, *e2*, *ju63*, *ju426*, *e116*, *ju22*, *e1063*, *qa2211)*, *ephx-1(ok494)*, *tag-341(ok1498)*, *age-1 (hx546)*, *shc-2(tm328)*, and *cog-1(sy275)*; LGIII: *ina-1 (gm144)*, and *mig-10(ct41)*; LGIV: *efn-1(e96*, *ju90)*, *efn-2 (ev658)*, *arf-6(tm1447)*, *daf-18(ok480)*, *rga-5(ok2241)*, *jac-1(ok3000)*, and *ngn-1(ok2200)*; LGV: *akt-1(ok525)*; *lsy-6(ot71)*; *fmi-1(tm306)*; and LGX: *efn-3(ev696)*, *abl-1 (ok171)*, *sax-3(ky123)*, *git-1(tm1962)*, *gap-2(tm748)*, *nck-1(ok694)*, *wrk-1(ok695)*, *trk-1(tm3985*, *tm4054)*, *akt-2 (ok393*, *tm812)*, *unc-6(ev400)*, *sgk-1(ok538*, *ft15)*, and *pdk-1 (mg142*, *sa709)*. New *vab-1* alleles are listed in Table 1. Published transgenes are as follows: P*str-1*-GFP (*kyIs104*) (Troemel *et al.* 1997); P*str-3*-GFP (*kyIs128*) (Zallen *et al.* 1999), P*gcy-5*-GFP (*ntIs1*) (Altun-Gultekin *et al.* 2001), P*gcy-7*-GFP (*otIs3*) (Chang *et al.* 2003), P*gcy-8*-GFP (*oyIs17*) (Satterlee *et al.* 2001), and P*vab-1*-Venus (*evIs190*) (Ikegami *et al.* 2012).

### *Scoring of amphid axon guidance and dendrite extension*

To visualize amphid neuron morphology, we used dye filling (Hedgecock *et al.* 1985). To visualize individual neurons, we

**Table 1 Phenotypic strength of selected *vab-1* mutations and molecular lesions**

| Allele | Mutagen | Embryonic lethality (%) | Larval lethality (%) | Adult, Vab (%) | Adult, non-Vab (%) | WT sequence | Mutant sequence | Effect |
|---|---|---|---|---|---|---|---|---|
| Strong | | | | | | | | |
| *e2027(null)* | SPO | 58.2 | 31.3 | 8.9 | 2.5 | — | 74-bp deletion, removing first 7 bp of exon 5 | — |
| *e721* | EMS | 58.2 | 29.3 | 11.4 | 1.0 | ACG | ATG | ATG codon in 5′-UTR |
| *ok1699* | UV | 53.4 | 20.7 | 23.9 | 2.0 | — | 1016-bp deletion of exon 5 | — |
| *ju220* | UV/TMP | 45.4 | 15.0 | 34.6 | 5.1 | — | Exon 1 rearrangement | — |
| *ju307* | EMS | 41.9 | 27.2 | 29.1 | 1.8 | GAA | AAA | E62K |
| Intermediate | | | | | | | | |
| *ju275* | EMS | 18.0 | 7.3 | 65.0 | 9.8 | GCG | GTG | A245V |
| Weak | | | | | | | | |
| *zd118* | EMS | 13.8 | 7.5 | 24.6 | 54.0 | TGG | TGA | W934opal |
| *ju426* | EMS | 13.6 | 2.1 | 55.3 | 28.9 | TGG | TGA | W934opal |
| *e118(kd)* | EMS | 10.1 | 8.6 | 45.6 | 35.8 | — | 326-bp deletion in exon 10 | — |
| *ju306* | ENU | 1.7 | 1.4 | 32.4 | 64.4 | GTC | GAC | V220D |
| *qa2211* | EMS | 1.5 | 1.1 | 18.7 | 78.7 | GGA | GAA | G256E |

Three new alleles were characterized as genetically null based on phenotypic strength and molecular lesions: *ju220* is a rearrangement of unknown structure that affects exon 1, encoding the start codon and signal sequence; *ok1699* is a 1016-bp deletion of exon 5, which encodes part of the ephrin binding domain and the cysteine-rich domain in the extracellular domain; and *ju307* results in the same missense alteration (E62K) as the previously described *ju8* (George *et al.* 1998). The previously unsequenced null allele *e721* creates a premature ATG in the *vab-1* 5′-untranslated region; translation from this out-of-frame upstream ORF likely interferes with translation from the native *vab-1* ATG. Three new alleles result in missense alterations in the extracellular cysteine-rich domain, providing mutational evidence for the importance of this domain.

used transgenic markers labeling single amphid neuron types. We immobilized L4 stage hermaphrodites using 1% phenoxy-1-propanol in M9 and scored neuronal morphology using compound microscopy. For most genotypes, we scored >50, typically 100–200 neurons; genotypes for which <50 neurons were scored are indicated in the bar charts. In the wild type, essentially 100% of amphid axons extend ventrally in the commissure and then turn anteriorly into the nerve ring. We classified amphid axon guidance as normal, lateral, or other. The "other" category was rare (<5%) and only used if no axon was visible. As far as possible, we scored the initial guidance of the axon even if it changed direction subsequently; such changes in direction were rare. For screening, mutations were crossed into the *vab-1(e118)* kinase-dead background. To assess significance of differences in proportions we used the Fisher exact test or the chi-squared test.

### *Transgenic rescue of vab-1 and efn-1 phenotypes*

To assess rescue of the *vab-1* phenotypes, transgenic lines containing *vab-1* genomic cosmid DNA (M03A1; pRF4 coinjection marker) (George *et al.* 1998), fosmid DNA (WRM0617bA10 in *juEx2870*) or the rescuing VAB-1::GFP minigene (pCZ55) (George *et al.* 1998) were generated. These lines were crossed into the *vab-1(e2027); kyIs104* background and scored for rescue of guidance defects. Similarly, a transgene containing wild-type *efn-1* genomic DNA (pCZ126), as well as a rescuing GFP::EFN-1 fusion (pCZ131 in *juIs52*) (Chin-Sang *et al.* 1999) were crossed into the *efn-1(e96); kyIs104* mutant background.

### *Tissue-specific rescue experiments*

We amplified full-length coding sequences and 3′-UTRs from cDNA clones yk497d6 (VAB-1A), yk338g11 (EFN-1), yk708d1 (EFN-2), yk1482h02 (ABL-1A), and cloned them into pCR8 to create Gateway entry clones pCZGY1146, pCZGY1145, pCZGY1148, pCZGY1835, and pCZGY1834. All entry clones were sequenced. We used the following tissue-specific promoters: *unc-33* and *rgef-1* (Altun-Gultekin *et al.* 2001), *unc-119* (Maduro and Pilgrim 1995), *myo-2* (Frøkjaer-Jensen *et al.* 2006), *ttx-3* (Hobert *et al.* 1997), *dyf-7* (Heiman and Shaham 2009), *lin-26* (Labouesse *et al.* 1994), *str-1* (Troemel *et al.* 1997), and *hlh-17* (Yoshimura *et al.* 2008). After recombination with entry vectors containing the desired cDNA, final constructs were injected into wild-type (N2) worms at 1 ng/μl together with 15 ng/μl *sur-5*-mCherry as a coinjection marker; see Supporting Information, Table S1 for a list of clones and transgenes. Each transgene was crossed into the relevant mutant background; at least two transgenes per construct were scored, and representative lines are reported.

### *Expression analysis*

To determine cellular expression patterns of VAB-1 and EFN-1, we examined animals expressing the rescuing transgenes *juIs24* (VAB-1::GFP), *juIs52* (EFN-1::GFP), and the *vab-1* transcriptional reporters *juEx101* and *evIs190*. To examine fixed animals, we performed fixation and staining as described (Finney and Ruvkun 1990). Fixed animals were incubated with rabbit anti-GFP polyclonal (A11122, Invitrogen, 1:1000 dilution) and mouse anti-AJM-1 monoclonal (MH27, 1:500) overnight at 4° and staining visualized with appropriate 2° antibodies.

### *4D lineage analysis of EFN-2 expression*

To examine *efn-2* embryonic expression, we generated the transgene P*efn-2*-HIS-24::mCherry::*let-858* 3′-UTR (*juEx2737*), which contains 2.7 kb of *efn-2* upstream sequence. We followed

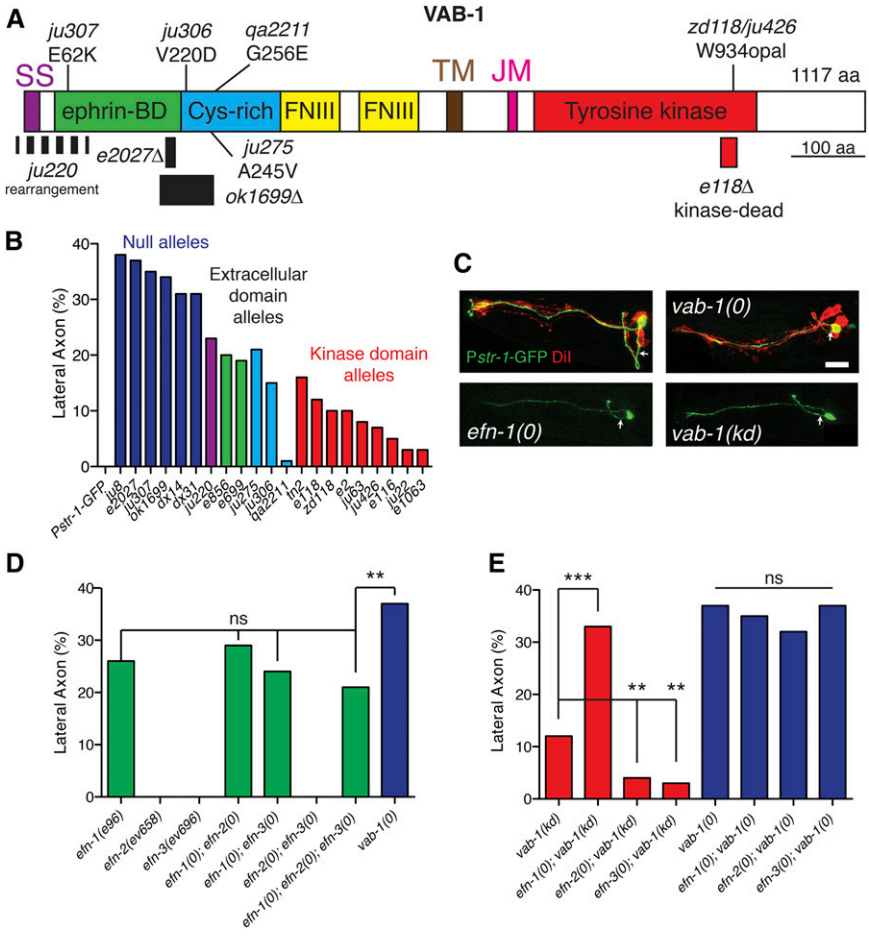


**Figure 1** Ventral guidance of amphid commissure axons is dependent on EFN-1-VAB-1 signaling. (A) Domains of VAB-1 and locations of molecular lesions. Previously isolated deletion alleles *e2027 (null)* and *e118(kd)* are included for reference. *ok1699* is a deletion and *ju220* is a rearrangement of unknown structure. SS, signal sequence; TM, transmembrane domain; JM, juxtamembrane domain. (B) Quantitation of AWB guidance defects in Eph receptor null mutants (*ju307*, *ju8*, *e2027*, *ok1699*, *dx14*, and *dx31*), extracellular domain alleles (*ju220*, *ju275*, *e856*, *e699*, and *ju306*), and kinase dead alleles (*tn2*, *e118*, *zd118*, *e2*, *ju63*, *e116*, *ju22*, and *e1063*). Color coding corresponds to region of protein affected by mutation. (C) Amphid axon guidance in *vab-1* and *efn-1* mutants; AWB (P*str-1*-GFP, green) and DiI staining (red). Confocal projections, anterior is left and dorsal is up. Arrows indicate axon extending from cell body. Bar, 10 μm. (D) Quantitation of AWB guidance defects in *efn* mutants and double mutants. Asterisks indicate compound mutants significantly different from the *efn-1* single mutant. (E) Quantitation of guidance defects in double mutants between each ligand and the *vab-1(e118)* kinase dead receptor strain or double mutants between each ligand and the receptor null *vab-1(e2027)*. $N > 50$ neurons per genotype in this and all subsequent bar charts, except where $N$ is indicated in the bar. Statistics, Fisher exact test: $^{*}P < 0.05$; $^{**}P < 0.01$; $^{***}P < 0.001$.

its expression in a HIS-72::GFP (*zuIs178*) background and identified P*efn-2*-mCherry-expressing cells in two embryos using 4D confocal microscopy and the lineaging software NucleiTracker4D (Giurumescu *et al.* 2012).

### *Analysis of new vab-1 alleles*

In addition to previously described *vab-1* alleles (George *et al.* 1998), we characterized eight additional alleles (Table 1; Figure 1A). Mutations *ju307*, *ju275*, *zd118*, *qa2211*, and *ju426* were isolated based on epidermal morphology phenotypes after EMS mutagenesis. *ju306* was isolated after ENU mutagenesis and *ju220* was recovered after UV/Trimethylpsoralen (TMP) mutagenesis. *ok1699* was isolated following UV mutagenesis by the *C. elegans* Gene Knockout Consortium. DNA lesions were determined by exon sequencing and penetrance determined as described (George *et al.* 1998).

## Results

### *Amphid ventral guidance involves both kinase-dependent and kinase-independent functions of VAB-1/Eph receptor*

Amphids are sensory organs containing 12 bilaterally symmetric pairs of neurons whose cell bodies are located in the lateral ganglia of the head. Amphid neuron cell bodies are born in the anterior head in midembryogenesis, move anteriorly to anchor their dendrite tip, then migrate posteriorly, laying down their sensory processes by "retrograde extension" (Sulston *et al.* 1983; Heiman and Shaham 2009). Once the amphid cell body reaches its final place in the lateral ganglia, the amphid axons grow out ventrally then turn and extend anteriorly and dorsally into the nerve ring. Amphid axons are fasciculated in their ventral trajectories, forming two bundles known as the amphid commissures. Previous work revealed that amphid commissure guidance was strongly dependent on VAB-1/EphR signaling: *vab-1(dx31)* null mutants display 30–40% guidance defects in which amphid axons leave the cell body laterally and enter the nerve ring without following the normal ventral trajectory (Zallen *et al.* 1999). Defects were significantly less penetrant in the kinase-dead allele *vab-1(e2)*, suggesting amphid axon guidance is a suitable model for VAB-1/EphR kinase-independent signaling.

To confirm the requirement for VAB-1, we examined amphid axon guidance in the entire *vab-1* allelic series using the AWB marker P*str-1*-GFP (*kyIs104*) (Figure 1B). Axon guidance defect penetrance correlated strongly with penetrance of lethality or body morphology defects (Table 1; George *et al.* 1998). Putative *vab-1* null alleles (*e2027*, *dx31*, *ju8*, *ok1699*, *dx14*, and *ju307*) cause between 31

and 38% axon guidance defects, whereas likely kinase-dead *vab-1* alleles (*e118*, *e2*, and *zd118*) display 10% defects. The penetrance of defects in *vab-1(e2027)* L1 stage animals was comparable to that observed in L4 animals (not shown), suggesting guidance errors arise during initial amphid axon outgrowth in embryogenesis and do not result from a failure to maintain axon position. These results confirm that both kinase-dependent and kinase-independent VAB-1 functions are involved in amphid axon guidance. Hereafter we refer to the reference null *vab-1(e2027)* as *vab-1(0)*, and to the reference kinase dead allele *vab-1(e118)* as *vab-1(kd)*. In agreement with previous observations (Zallen *et al.* 1999), *vab-1* mutations affect all amphid axons equally; guidance of the amphid axon bundle is typically either completely ventral or completely lateral. Below, we focus on a representative neuron, AWB.

### *Amphid axon guidance is dependent on EFN-1, which signals through both VAB-1 kinase-dependent and -independent pathways*

Previous studies had not resolved which ephrin ligands were involved in amphid axon guidance. We found that of the four *C. elegans* ephrins, only *efn-1(0)* mutants displayed amphid axon ventral guidance defects like those of *vab-1*, at lower penetrance (25%; Figure 1, C and D). These observations suggested that EFN-1 might be partly redundant with EFN-2 and EFN-3 in regulating ventral guidance. *efn-2* or *efn-3* null mutants or *efn-2 efn-3* double mutants displayed completely normal AWB guidance (Figure 1D). *efn-1 efn-2* and *efn-1 efn-3* double mutants resembled *efn-1* single mutants, as did the *efn-1 efn-2 efn-3* triple mutant (Figure 1D). Thus, EFN-1 is the major ephrin ligand involved in amphid axon guidance. As shown below, EFN-2 may play a minor role in guidance.

To address how EFN-1 may regulate VAB-1 signaling, we examined amphid guidance in *efn-1 vab-1* double mutants. The phenotype of *vab-1* null mutants was not enhanced by *efn-1(0)*, consistent with EFN-1 and VAB-1 acting in a linear pathway. We next addressed whether EFN-1 acted in the VAB-1 kinase-dependent or kinase-independent pathway by examining double mutants between each ephrin ligand and the kinase dead receptor. We interpret enhancement of the kinase-dead phenotype as evidence for signaling in a kinase-independent pathway. *efn-1(0) vab-1(kd)* double mutants showed enhancement relative to *vab-1(kd)* but not to *efn-1(0)* alone, consistent with EFN-1 signaling at least in part through a kinase-independent pathway (Figure 1E). Conversely, *efn-2 vab-1 (kd)* and *efn-3 vab-1(kd)* mutants displayed significant suppression of axon guidance defects relative to *vab-1(kd)*, suggesting EFN-2 and EFN-3 have a cryptic function that antagonizes the kinase-independent pathway. *efn-2* or *efn-3* neither enhanced nor suppressed *vab-1(0)* guidance defects, implying that the antagonistic effects of EFN-2/3 require the Eph receptor (Figure 1E).

To test whether loss of EFN-2 improved VAB-1 signaling by enhancing EFN-1 activity, we examined whether *efn-1* partial loss-of-function mutants could be suppressed by *efn-2(lf)* and found no significant suppression in these double mutants (not shown). Loss of EFN-2 may be unable to compensate for the reduced EFN-1 function in these mutants. To address the specificity of *efn-2* suppression, we analyzed double mutants between *efn-2* and the netrin receptor *unc-40* or *sax-3*/Robo. *efn-2* weakly suppressed guidance defects in both cases (not shown), although this was not statistically significant. These data imply that loss of *efn-2* function might increase EFN-1/VAB-1 signaling via VAB-1, resulting in slight improvement of guidance in the absence of UNC-40 or SAX-3.

### *VAB-1 is expressed and required in amphid neurons for axon guidance*

We considered two general models for how VAB-1 and EFN-1 might promote amphid guidance (Figure 2A). First, VAB-1 in amphid neurons might interact with EFN-1 on surrounding guidepost cells, mediating a receptor-dependent forward signal into axons. EFN-1 might present an attractive cue on ventral guidepost cells or EFN-1 might repel amphid axons from the more lateral pathway; the stereotyped lateral guidance of aberrant axon trajectories in *vab-1*, *unc-40*, or *sax-3* suggests that the lateral path represents a "default" pathway for axons in the absence of ventral cues. In the second model EFN-1 in amphid neurons might interact with VAB-1 in surrounding cells, mediating an ephrin reverse signal into axons. More complex models in which VAB-1 and EFN-1 are coexpressed in amphids and surrounding cells are also possible.

VAB-1 is widely expressed in anterior neurons during embryonic and larval development (George *et al.* 1998; Brisbin *et al.* 2009). During larval stages P*vab-1*-GFP expression becomes more restricted, and was observed strongly in at least one amphid neuron pair, ASIR/L (Figure 2B). We therefore focused on testing the cellular requirement of VAB-1 using a variety of tissue- or cell-specific promoters (Table S1). We verified that the *vab-1(0)* axon guidance phenotypes were fully rescuable by genomic *vab-1* DNA or by the VAB-1::GFP transgene (George *et al.* 1998). Expression of VAB-1 under the control of early panneuronal promoters such as *unc-33* partly rescued *vab-1(0)* phenotypes from 38 to 27%, suggesting expression of VAB-1 in neurons is sufficient to promote normal amphid guidance; expression under the control of the later-onset *rgef-1* promoter did not significantly rescue, suggesting VAB-1 expression later in neuronal differentiation is not sufficient. When we expressed VAB-1 using an amphid (P*dyf-7*) or AWB-specific promoter (P*str-1*), *vab-1(0)* mutant phenotypes were significantly rescued (18–28%; Figure 2C). In contrast, expression of VAB-1 from nonneuronal promoters, including *lin-26* (glial and epidermal cells), *hlh-17* (cephalic sheath cells), or *myo-2* (pharyngeal muscle), did not rescue amphid axon defects. Taken together, our expression and tissue-specific rescue experiments are most consistent with VAB-1 acting directly in amphid neurons to promote axon guidance.

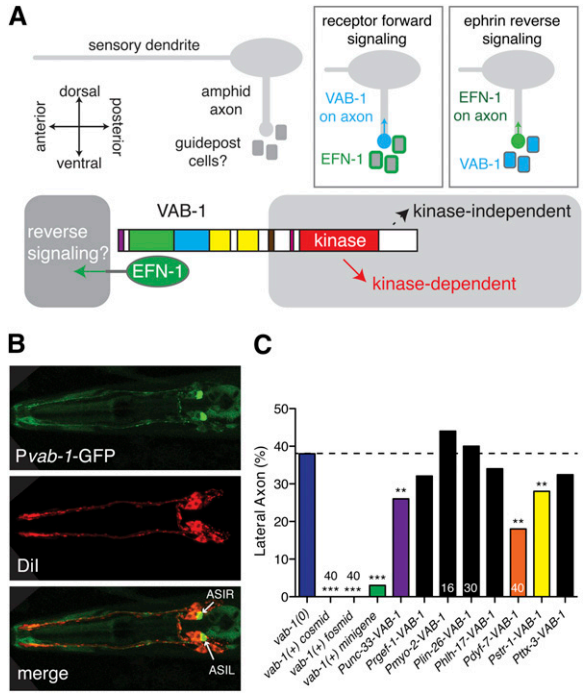


**Figure 2** Expression and tissue-specific rescue of VAB-1. (A) Models for the cellular focus of VAB-1 and ephrins in amphid axon ventral guidance. (B) P*vab-1*-GFP (*evIs190*) expression in amphid neurons, including ASI, and in nerve ring in larvae. Anterior is to the left, dorsal views. ASI is identified as the most posterior of the dorsal trio of large amphid neurons, double labeled with DiI (red). (C) Tissue and cell-specific rescue of *vab-1* guidance defects. All transgenic rescue assays were conducted in *vab-1(e2027); kyIs104* mutant background. Asterisks indicate significant differences from *vab-1* single mutant by Fisher exact test: $*P < 0.05$; $**P < 0.01$; $***P < 0.001$.

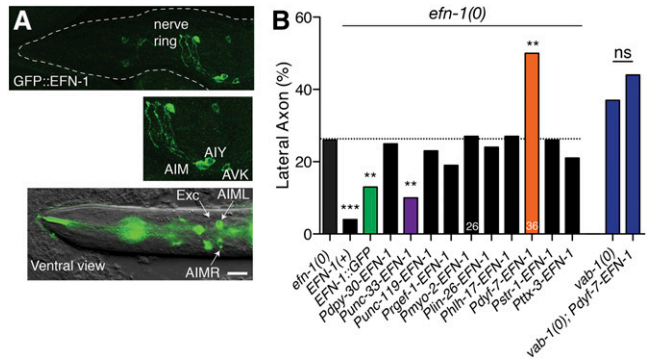


**Figure 3** EFN-1 expression and tissue-specific rescue. (A) EFN-1::GFP (*juIs52*) expression in larvae and adults. EFN-1::GFP is expressed in a small number of anterior neurons, identified based on position and morphology as AIM, AIY, and AVK. (B) Tissue and cell-specific rescue of *efn-1* axon guidance defects, scored in the *efn-1(e96); kyIs104* background or in *vab-1(e2027)* as indicated. Asterisks indicate significant difference from *efn-1* single mutant defects, by Fisher exact test. $N > 50$ except where indicated. $*P < 0.05$; $**P < 0.01$; $***P < 0.001$. Bar, 10 μm.

### *EFN-1 is expressed and required in neurons and may interfere with VAB-1 when misexpressed in amphid neurons*

EFN-1::GFP is expressed widely in anterior neurons in midembryogenesis (Chin-Sang *et al.* 1999), but like VAB-1 becomes more restricted during larval stages. In larvae, EFN-1::GFP was not observed in amphid neurons but was seen in a set of ventral neurons including AIM, AIY, and AVK (Figure 3A). Tissue-specific expression of EFN-1 under the control of the panneuronal *unc-33* promoter significantly suppressed *efn-1(0)* guidance defects, suggesting EFN-1 is at least partly required in neurons. However, amphid-specific expression of EFN-1 strongly enhanced guidance defects in an *efn-1(0)* mutant (Figure 3B). We reasoned that if EFN-1 is not normally expressed in VAB-1-expressing amphid neurons, its ectopic expression in amphid neurons could inhibit VAB-1 signaling by a *cis*-interaction similar to that reported between ephrin-A5 and EphA3 in retinal axons (Carvalho *et al.* 2006). Consistent with this hypothesis, P*dyf-7*-EFN-1 did not significantly enhance guidance defects of a *vab-1(0)* mutant. Thus, ventral guidance defects due to misexpression of EFN-1 may reflect inhibition of VAB-1/EphR in amphid neurons. As the P*dyf-7*-EFN-1 guidance defects in an *efn-1(0)* background are slightly more severe than those of *vab-1(0)*, EFN-1 overexpression may also interfere with the function of SAX-3 or UNC-40, which are known to be expressed in amphid neurons (Chan *et al.* 1996; Zallen *et al.* 1998). Expression of EFN-1 under the control of nonneuronal or AWB-specific promoters (*lin-26*, *hlh-17*, *myo-2*, or *str-1*) neither rescued nor enhanced *efn-1* phenotypes. Overall these data are consistent with EFN-1 functioning in nonamphid neurons, presumably guidepost cells for amphid axons.

### *Eph signaling in amphid axon guidance displays left–right asymmetry*

In the course of analyzing amphid ventral guidance phenotypes, we noticed that almost all *vab-1* and ephrin mutant strains displayed a strong left–right bias, in that guidance defects were two to four times more frequent in the left-hand neuron of a bilateral pair (Figure 4, A and B). Such asymmetric guidance defects were seen in multiple singly labeled neuron types and in amphid neurons labeled by dye filling. In contrast, the penetrance of guidance defects in *unc-40* (Netrin receptor) or *sax-3* (Robo) mutants did not display left–right bias (Figure 4B). Thus, despite the overt symmetry of axon guidance in the wild type, left-hand neurons are more dependent on Eph signaling than are right-hand neurons.

Amphid neurons are known to display left–right asymmetries in gene expression and function, determined cell autonomously by gene regulatory cascades (Hobert *et al.* 2002; Johnston and Hobert 2003). To distinguish whether an amphid neuron's identity or its environment determines the asymmetric response to loss of ephrin signaling, we used *lsy-6* mutants, in which a left-hand neuron (ASEL) is genetically transformed into its right-hand counterpart ASER (Johnston and Hobert 2003). If left-hand bias in guidance defects reflects an intrinsic aspect of the ASEL fate, ASER

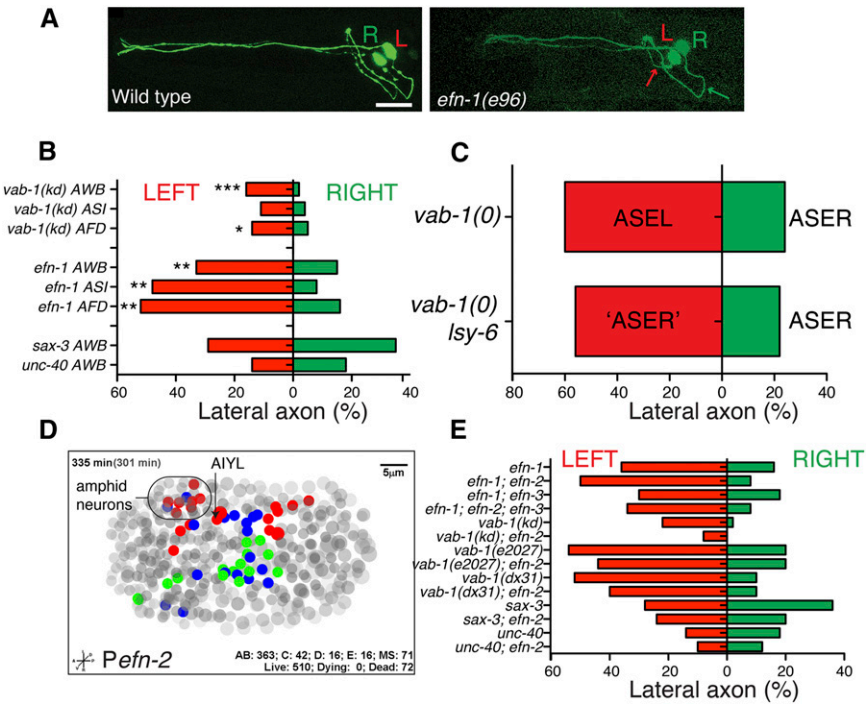


**Figure 4** Ephrin signaling has asymmetric requirements in amphid commissure ventral guidance. (A) Amphid outgrowth defects display left-hand bias in Eph signaling mutants; representative example from *efn-1(e96)*. Bar, 10 μm. (B) Quantitation of axon guidance defects in left *vs.* right hand AWB, ASI, or AFD axons in *efn-1* or *vab-1(e118)* mutants. *unc-40* and *sax-3* do not show detectable left–right bias in penetrance. Green bars are right-side axons and red bars, left. (C) Transformation of ASEL into an ASER-like fate by *lsy-6* does not alter the left-hand bias in guidance defects in *vab-1 (e2027)* background. (D) Asymmetry in P*efn-2*-mCherry (*juEx2737)* expression as determined by 4D lineage analysis at 335 min postfertilization; anterior is to the left and left is up. Blue nuclei are bilateral pairs that show symmetrical expression of *efn-2*, green nuclei are members of bilateral pairs for which only the right-hand side expresses *efn-2*, red nuclei are members of pairs that express only on the left-hand side. Gray nuclei are nonexpressing (grayscale depth code). See Table S2 for list of expressing nuclei. (E) Loss of *efn-2* function increases asymmetry of *efn-1* mutants, does not affect *vab-1(e2027)* or *vab-1(dx31)* null mutants, and decreases penetrance and asymmetry in *vab-1(kd)*.

should not show higher guidance defects when on the left side. However if the left-side environment determines reliance on Eph signaling then the transformed ASER (left) should show enhanced defects compared to the nontransformed ASER (right). In *vab-1(0) lsy-6* double mutants we observed a strong left-hand bias in defects ($P < 0.01$), equivalent to that in *vab-1(0)* alone (Figure 4C), suggesting it is not the lateralized identity of the cell, but a difference in the environment that leads to the asymmetry of Eph guidance defects.

Our analysis of VAB-1 and EFN-1 expression patterns did not reveal overt left–right asymmetries in amphid neurons or surrounding cells. We therefore examined the embryonic expression of EFN-2 using 4D lineage analysis of an *efn-2* transcriptional reporter. We found that *efn-2* expression shows widespread left–right asymmetry in embryos, both in amphid neurons and in other cells (Figure 4D; Table S2). This asymmetry involves expression in either the right or left member of a bilaterally symmetrical neuron pair. The asymmetric expression of *efn-2* prompted us to reexamine whether *efn-2* mutants might have subtle asymmetric effects on amphid guidance that were not evident from averaging defects on both sides. Loss of function in *efn-1* causes a strong left-hand bias in defects that is exacerbated in *efn-1 efn-2*: defects on the left side increase from 36 to 50%, and defects on the right side decrease from 16 to 8% (Figure 4E), resulting in slightly increased overall defects (Figure 1D). In contrast, loss of *efn-2* improves left-hand guidance in *vab-1(kd)* mutants, suggesting the effect of EFN-2 on left-side guidance can be positive or negative depending on the presence of EFN-1. Loss of *efn-2* function did not modify the left–right bias of defect in *vab-1(0)* consistent with the idea that the inhibitory effect of EFN-2 requires VAB-1. Asymmetric expression of EFN-2 or other guidance cues could contribute to the unequal roles of Eph signaling in left and right amphid axon guidance.

### *Screening candidates for components of Eph signaling in axon guidance*

To identify additional components of Eph signaling involved in axon guidance, we screened candidate genes chosen based on their involvement in Eph signaling in other tissues or organisms (Table 2). We scored guidance in all single mutants and selected mutants in the *vab-1(kd)* and *vab-1 (0)* backgrounds, reasoning that mutations affecting a VAB-1 kinase-independent pathway should enhance *vab-1 (kd)* but not *vab-1(0)*. VAB-1 kinase-independent signaling could potentially act downstream of VAB-1 in a "forward" pathway, or in a "reverse" pathway into the EFN-1-expressing cell. Loss of function in candidate coreceptors for ephrin reverse signaling such as the TrkB homolog *trk-1* (Manning 2005) did not affect guidance. Other potential VAB-1 ligands such as the atypical ephrin EFN-4, VPR-1, or the Wrapper/Klingon-like receptor WRK-1 did not affect amphid axon guidance as single mutants and were not tested further (Table 2). Some sterile or maternal-effect mutants, such as *src-1* were only tested as single mutants and did not affect guidance. Loss of function in *mig-10*/Lamellipodin or in *ngn-1*/Neurogenin caused highly penetrant axon guidance defects as single mutants and may affect parallel pathways or multiple signaling pathways. Most single mutants did not display axon guidance defects and did not modify the *vab-1 (kd)* phenotype, including several genes implicated in Eph signaling in other contexts, such as *nck-1*/Nck or *ephx-1/*

**Table 2 Candidate Eph signaling genes in *C. elegans***

| | Single mutant lateral axon phenotype (%) | Double *vab-1(kd)* mutant lateral axon phenotype (%) | Compound *vs. vab-1 (kd)* (*P*-value) | Mammalian homolog |
|---|---|---|---|---|
| *vab-1(e118)* | — | 12 | — | |
| Class I: suppressors of *vab-1(kd)* | | | | |
| *akt-1(ok525)* | 0 | 3 | ***0.0009, *N* = 200 | Akt/PKB |
| *sgk-1(ok538)* | 0 | 3 | **0.002, *N* = 160 | SGK/serum-and glucocorticoid-inducible kinase |
| *daf-16(mu86)* | 0 | 3 | **0.003, *N* = 200 | FOXO |
| *efn-3(ev696)* | 0 | 3 | **0.008, *N* = 134 | Ephrin-A ligands |
| *efn-2(ev658)* | 0 | 4 | **0.006, *N* = 268 | Ephrin-A ligands |
| *egl-19(ad695gf)* | 0 | 4 | *0.024, *N* = 164 | VGCC α subunit |
| *daf-18(ok480)* | 0 | 4 | *0.036, *N* = 100 | PTEN |
| Class II: specific enhancers of *vab-1(kd)* | | | | |
| *efn-1(e96)* | 26 | 33 | ***0.0001, *N* = 122 | Ephrin-A ligands |
| *abl-1(ok171) 25°* | 0 | 32 | **0.002, *N* = 100 | Abl/Abelson kinase |
| *abl-1(ok171)* | 1 | 22 | 0.091, *N* = 100 | Abl/Abelson kinase |
| *aap-1(m889) 25°* | 0 | 28 | *0.041, *N* = 50 | PI3K *p50/p55* |
| *age-1(hx546) 25°* | 0 | 22 | 0.06, *N* = 130 | PI3K *p110* |
| Class III: nonspecific enhancers of *vab-1(kd)* | | | | |
| *ngn-1(ok2200)* | 32 | 50 | ***0.0001, *N* = 100 | Neurogenin |
| *mig-10(ct41)* | 2 | 22 | *0.05, *N* = 200 | Lamellipodin |
| Class IV: no significant change | | | | |
| *ina-1(gm144)* | 3 | 11 | 0.825, *N* = 100 | alpha integrin subunit |
| *git-1(tm1962)* | 0 | 8 | 0.355, *N* = 100 | GIT1 |
| *arf-6(tm1447)* | 0 | 11 | 0.825, *N* = 100 | ARF6 |
| *nck-1(ok694)* | 0 | 14 | 0.834, *N* = 100 | NCK adapter protein |
| *shc-1(ok198)* | 0 | 8 | 0.347, *N* = 100 | Shc proteins |
| *shc-2(tm328)* | 1 | — | — | Shc proteins |
| *ephx-1(ok494)* | 0 | 15 | 0.683, *N* = 100 | Ephexin |
| *rga-5(ok2241)* | 0 | 12 | 1.0, *N* = 100 | Rho GTPase Activating protein |
| *gap-2(tm748)* | 0 | — | — | nGAP/synGAP |
| *vpr-1(tm1411)* | 0 | — | — | VAPB |
| *wrk-1(ok695)* | 0 | 9 | 0.490, *N* = 100 | Wrapper/Rega-1/Klingon |
| *trk-1(tm3895)*†† | 0 | 14 | 0.822, *N* = 72 | TRK neurotrophin receptor |
| *trk-1(tm4054)*†† | 0 | 6 | 0.139, *N* = 100 | TRK neurotrophin receptor |
| *src-1(cj293)* | 0 | — | — | Src family kinase member |
| *src-2(ok819)* | 0 | 12 | 1.0, *N* = 50 | Src family kinase member |
| *egl-19(n2368cs)* | 4 | 6 | 0.138, *N* = 100 | VGCC α subunit |
| *jac-1(ok3000)* | 0 | 5 | 0.125, *N* = 100 | *p120* catenin |
| *tag-341(ok1498)* | 1 | 5 | 0.056, *N* = 200 | F-BAR and RhoGAP domains |
| *akt-2(ok393)* | 0 | 14 | 0.836, *N* = 100 | Akt/PKB |
| *akt-2(tm812)* | 0 | 18 | 0.326, *N* = 100 | Akt/PKB |
| *lsy-6(ot71)* | 0 | 19 | 0.248, *N* = 100 | N/A |
| *cog-1(sy275)*† | 5 | — | — | Nkx6 homeodomain protein |
| *wsp-1(gm324)* | 0 | 10 | 0.652, *N* = 100 | N-WASP |
| *goa-1(sa734)* | 1 | Sterile | — | Heterotrimeric G protein alpha subunit Go (Go/Gi class) |
| *fmi-1(tm306)* | 7 | — | — | Celsr/Flamingo |
| *efn-4(bx80)* | 3 | — | — | Ephrin-A ligands |

*N*, number of neurons scored. †*cog-1* was tested with the P*gcy-7*-GFP marker to label ASEL. ††*trk-1(tm3985)* is a 176-bp deletion, which removes most of exons 8 and 9 of the primary sequence and is predicted to truncate the protein between the transmembrane and kinase domain. *tm4054* is an 823-bp deletion, which removes exons 6–9 and is predicted to be a null. Statistics, Fisher exact test: *, $P < 0.05$, **, $P < 0.01$, ***, $P < 0.001$.

Ephexin. Below we focus on two pathways that displayed specific roles in amphid guidance: the PI3-kinase/Insulin signaling pathway and the nonreceptor tyrosine kinase *abl-1*/Abl.

### *PI3-kinase signaling promotes amphid axon guidance*

The phosphatidylinositol 3-kinase pathway plays widespread roles in Eph signaling; in *C. elegans*, VAB-1 promotes PI3K signaling in neurons by negatively regulating the phosphatase DAF-18/PTEN (Brisbin *et al.* 2009). We therefore tested *age-1* and *aap-1*, which encode the *C. elegans* orthologs of the PI3K p110 catalytic and p50/p55 adaptor/regulatory subunits. *age-1* or *aap-1* single mutants displayed normal amphid guidance and both significantly enhanced the *vab-1(kd)* phenotype (Figure 5A). Loss of *aap-1* or *age-1* also enhanced *efn-1(0)* guidance defects, and *age-1*

enhanced *vab-1* null mutant defects. PI3K signaling has recently been shown to cell-autonomously promote axon outgrowth of the AIY neuron (Christensen *et al.* 2011); we found that AWB also displayed outgrowth defects in PI3K mutants, but that these were independent of axon guidance or VAB-1 (not shown). These results suggest PI3-kinase signaling promotes amphid guidance and that loss of VAB-1 function sensitizes amphid axons to loss of PI3K activity. As *vab-1(0)* is enhanced by PI3K mutations, PI3K acts in parallel to VAB-1. An additional role for PI3K downstream of VAB-1 cannot be excluded.

*daf-18* encodes the *C. elegans* PTEN phosphatase that acts antagonistically to PI3K (Ogg and Ruvkun 1998). VAB-1 has been shown to interact with and negatively regulate PTEN expression and function in amphid neurons in a kinase-dependent manner (Brisbin *et al.* 2009). We found that *daf-18 vab-1(kd)* mutants showed significant suppression of amphid guidance defects, consistent with PI3K signaling promoting guidance (Figure 5B). Loss of function in *daf-18* did not suppress amphid axon guidance defects of *unc-40* null mutants, suggesting loss of *vab-1* kinase activity might sensitize axons to levels of PI3K signaling. In the course of these experiments, we observed that *daf-18* displayed strong synergistic lethality with *vab-1* or *sax-3* null mutants (not shown). Analysis of a limited number of surviving *vab-1(0) daf-18* double mutants revealed slight enhancement of guidance defects that was not statistically significant. Thus, DAF-18 may play both positive and negative roles in guidance depending on the signaling context.

In *C. elegans* PI(3,4,5)$P_3$ ($PIP_3$) is thought to act via a variety of kinases, including AKT-1/AKT-2 (Paradis and Ruvkun 1998) and PDK-1 (Paradis *et al.* 1999). The serum-and glucocorticoid-inducible kinase SGK-1 strictly depends on PDK-1 for its activation, but transduces $PIP_3$ signals by forming a complex with AKT-1/2 to control life span through regulation of DAF-16 (Hertweck *et al.* 2004). We therefore tested *pdk-1*/PDK, *sgk-1*/SGK, and the Akt/PKB homologs *akt-1* and *akt-2*. Unexpectedly, loss of function in each of these kinases except *akt-2* suppressed *vab-1(kd)* defects (Figure 5B). Loss of function in a target of the PI3-kinase/insulin pathway, DAF-16/FOXO (Lin *et al.* 1997; Ogg *et al.* 1997), also suppressed *vab-1(kd)* guidance defects.

Overall, these results further demonstrate that PI3K signaling influences amphid axon guidance but suggest that the roles of PI3K-dependent kinases may differ from their canonical roles as defined by their functions in aging or dauer formation (Paradis and Ruvkun 1998; Paradis *et al.* 1999; Hertweck *et al.* 2004). Reduced PI3K activity enhanced guidance defects, yet loss of function in the kinases that transduce $PIP_3$ activity suppressed guidance defects. These results suggest a more complex and possibly noncanonical relationship between VAB-1 and the PI3K pathway in axon guidance.

***The ABL-1 tyrosine kinase acts in Eph signaling in amphid axon guidance:*** *abl-1* mutants display a low penetrance (1%) lateral amphid axon phenotype and significantly enhanced *vab-1(kd)*, but not *vab-1(0)* guidance defects (Figure 6A), suggesting *abl-1* acts in Eph signaling but independent of the Eph kinase. *abl-1 unc-40* double mutants did not display genetic interactions, consistent with ABL-1 acting specifically in Eph signaling (Figure 6A). *efn-1 abl-1* double mutants displayed significant enhancement, suggesting that although ABL-1 acts within the Eph pathway it is not solely downstream of EFN-1 (Figure 6A). *age-1 abl-1* double mutants displayed normal guidance. However, the *abl-1 age-1 vab-1(kd)* triple mutant displayed 45% guidance defects, equivalent to or slightly stronger than *vab-1(0)* (Figure 6B). This synergistic effect in the *vab-1(kd)* background suggests *abl-1* and *age-1* act in distinct pathways in amphid guidance, which are redundant with each other and with VAB-1 kinase-dependent signals.

To determine where ABL-1 functions in amphid axon guidance, we conducted tissue- and cell-specific rescue experiments. We expressed the ABL-1 cDNA under the

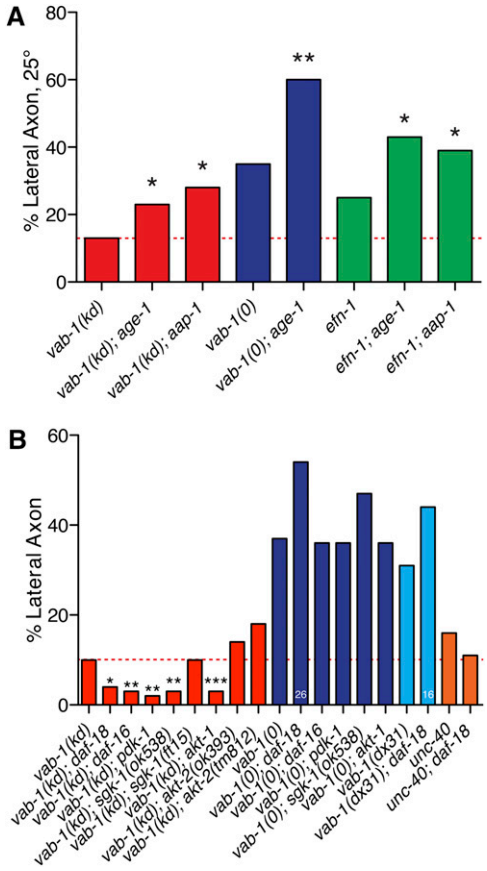


**Figure 5** Phosphatidylinositol 3-kinase signaling promotes amphid axon guidance. (A) Enhancement of *vab-1(kd)* amphid axon guidance defects by reduction of function in PI3-kinase activity. *age-1* and *aap-1* were tested at 25°. Significance is relative to the single *vab-1(kd)* mutant (red dashed line). (B) Loss of function in *daf-18*/PTEN, *daf-16*/FOXO, and in downstream PI3K signaling kinases suppresses *vab-1(kd)* guidance defects. *daf-18* slightly enhanced the ventral guidance defects of *vab-1* null mutants but this is not statistically significant; *daf-18* does not significantly affect *unc-40* penetrance. Statistics, Fisher exact test: $*P < 0.05$; $**P < 0.01$; $***P < 0.001$.

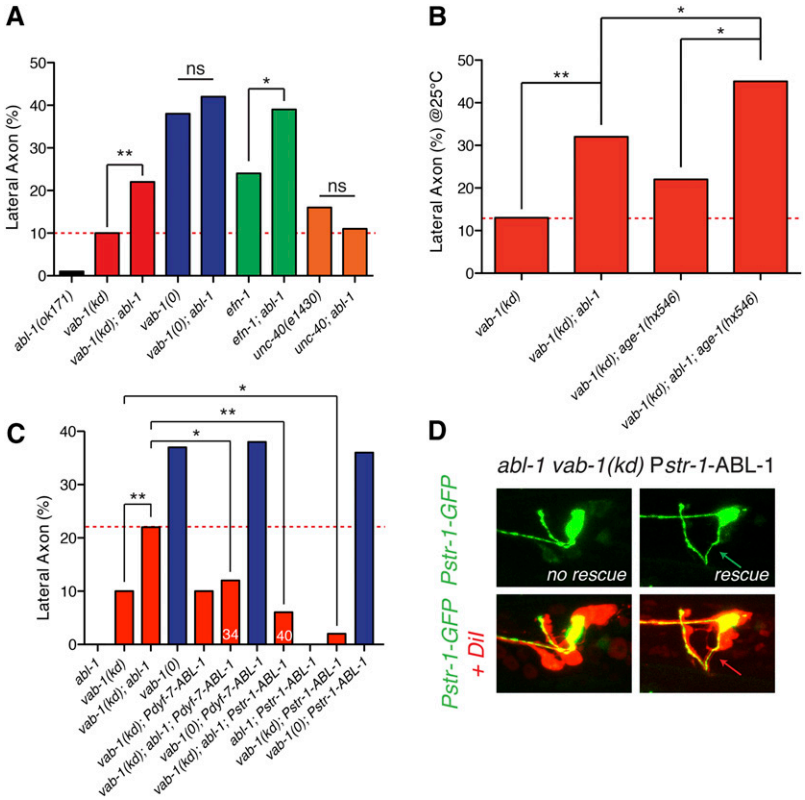


**Figure 6** ABL-1 signals in VAB-1-dependent amphid axon guidance. (A) Quantification of amphid axon guidance defects in *abl-1* mutants. (B) Synergism of guidance defects in the *vab-1(kd) abl-1 age-1* triple mutant suggests ABL-1 and PI3K act in parallel and are redundant with VAB-1 kinase signaling. (C) *dyf-7* driven (panamphid) expression of ABL-1 (*juEx4345*) rescues *abl-1* enhancement of *vab-1(kd)* guidance defects but not *vab-1(0)* defects. *str-1*-driven AWB-specific expression of ABL-1 (*juEx5059*) suppresses the *vab-1(kd) abl-1(ok171)* double mutant and the *vab-1(kd)* single mutant. (D) Rescue of guidance of multiple amphid axons by expression of ABL-1 in AWB. Images of *vab-1(kd); abl-1;* P*str-1*-ABL-1 *kyIs104* transgenic animals with other amphid axons visualized by DiI staining. Guidance of AWB correlates with guidance of other amphid axons in nonrescued and rescued animals ($N > 50$ axons). Statistics, Fisher exact test: $*P < 0.05$; $**P < 0.01$; $***P < 0.001$.

control of amphid-specific (*dyf-7*) or AWB-specific (*str-1*) promoters and tested for rescue of the *vab-1(kd) abl-1* enhanced phenotype. Amphid-specific expression of ABL-1 rescued the *vab-1(kd) abl-1* double mutant to the level of the *vab-1(kd)* phenotype alone, indicating ABL-1 acts in amphid neurons. Strikingly, expression of ABL-1 under the AWB-specific *str-1* promoter was able to suppress *vab-1(kd) abl-1* guidance defects to levels even lower than those of *vab-1(kd)* (Figure 6C). This suppression of *vab-1* by AWB-specific ABL-1 overexpression is also consistent with ABL-1 acting in AWB downstream of VAB-1. Moreover, when we examined other amphid neurons in both the P*str-1*-ABL-1 and P*str-1*-VAB-1 rescued lines, we found that rescue of AWB guidance was almost completely correlated with rescue of other axons in the commissure (Figure 6D; *vab-1* data not shown). Thus, AWB-specific expression of either ABL-1 or VAB-1 not only rescues AWB guidance but also rescues guidance of other amphid axons.

## Discussion

We were interested in the roles of Eph signaling in amphid axon guidance as a simple model for kinase-independent functions of Eph receptors. Our genetic and cellular analysis suggests the role of VAB-1 signaling in amphid axons is in several respects unlike its function in other cellular contexts in *C. elegans*. Thus, despite expressing a single Eph receptor and a small number of ephrin ligands, *C. elegans* Eph signaling is highly context specific (Miller and Chin-Sang 2012).

### *EFN-1 is the major ephrin promoting amphid axon ventral guidance*

In contrast to the previously characterized functional redundancy between EFN-1, EFN-2, and EFN-3 in embryonic morphogenesis and ventral neuroblast migration (Wang *et al.* 1999), only EFN-1 is required to properly guide the amphid axons and is sufficient to signal in the absence of EFN-2 and EFN-3. Unexpectedly, the *efn-1,-2,-3* triple mutant fails to phenocopy the *vab-1* receptor null in amphid guidance, suggesting that EFN-1,-2, and -3 do not collectively account for all VAB-1 activity. At least three explanations can be considered for this disparity between the *vab-1* null phenotype and the *efn-1,-2,-3* triple mutant. First, EFN ligands might antagonize one another. Removal of *efn-2* appears to slightly enhance *efn-1*, but this effect is negated by loss of *efn-3*. It is possible that EFN-3 acts in an inhibitory way to disrupt the functionality of EFN-1 or EFN-2 during ephrin signaling. We also find that loss of EFN-2 or EFN-3 mildly suppressed *vab-1(kd)*, suggesting EFN-2 and EFN-3 inhibit kinase-independent signaling. Loss of EFN-2 or EFN-3 does not affect the *vab-1* null phenotype, suggesting such suppression effect requires the VAB-1 receptor.

A second possibility is that amphid axon guidance involves an additional VAB-1 ligand. However, neither the fourth ephrin EFN-4 nor the nonephrin ligand VPR-1 appear to affect amphid axon guidance. Lastly, VAB-1 could have ligand-independent activity. In cancer cells EphB4 can regulate integrin-mediated adhesion independently of ephrin stimulation (Noren *et al.* 2009). In axon guidance, where

localized ligands give directional information, ligand-independent activity of VAB-1 might be permissive for other instructive signals such as netrins to promote ventral guidance.

### *Cellular sufficiency for Eph signaling in amphid axon guidance*

Our tissue-specific rescue experiments suggest VAB-1 functions at least in part in the nervous system, and most likely in the amphid neurons themselves. This conclusion is consistent with our expression data and previous evidence for VAB-1 functioning in amphid neurons (George *et al.* 1998; Brisbin *et al.* 2009). Conversely, EFN-1 does not appear to be expressed or required in amphid neurons; moreover, expression of EFN-1 in amphid neurons enhances the *efn-1(0)* mutant phenotype. We hypothesize that this enhancement reflects a *cis*-inhibitory interaction of EFN-1 and VAB-1, because amphid-specific expression of EFN-1 does not enhance *vab-1(0)*. Although we have not pinpointed the cells in which EFN-1 is expressed at the time of amphid guidance, it is noteworthy that EFN-1 is expressed in a set of ventral neurons, some of which are postsynaptic to amphid sensory neurons and whose cell bodies are close to the amphid commissure.

A caveat to our analysis is that none of our VAB-1 or EFN-1 tissue-specific transgenes fully rescued the corresponding mutant defects. As some panneural (*unc-33*) amphid (*dyf-7*) or AWB-specific (*str-1*) driven constructs had rescuing activity, these promoters appear to be expressed early enough to function during amphid axon guidance. We therefore suspect that the inability of transgenes to fully rescue *vab-1* or *efn-1* is because VAB-1 and EFN-1 are required either in multiple tissues or in a complex subset of neurons, and that panneural or panamphid expression does not sufficiently recapitulate these patterns.

### *VAB-1 and phosphatidylinositol 3-kinase signaling in axon guidance*

PI3K signaling is a key regulator of axon guidance in many organisms. In *C. elegans* ventral guidance of the AVM axon depends on AGE-1/PI3K to properly respond to UNC-6/netrin and SLT-1/slit cues (Chang *et al.* 2006). Eph receptors can physically interact with the p85 subunit of phosphatidylinositol 3-kinase (PI3K) (Pandey *et al.* 1994), as well as transmit kinase-independent forward signals through a PI3K pathway (Gu and Park 2001). In *C. elegans*, VAB-1 directly interacts with and inhibits PTEN in axon termination (Brisbin *et al.* 2009). Here we have shown genetic evidence that PI3-kinase signaling contributes to amphid axon guidance and may function in a VAB-1 kinase-independent manner. *vab-1(kd)* phenotypes are enhanced by loss of function in PI3K and suppressed by loss of function in DAF-18/PTEN. As *age-1* mutations enhance the *vab-1* null mutant PI3K signals do not solely act in the VAB-1 pathway and may also contribute to UNC-40- or SAX-3-dependent guidance or neuronal polarization, as in the AVM and HSN neurons (Adler *et al.* 2006; Chang *et al.* 2006). Nevertheless given the evidence for regulation of DAF-18 by VAB-1 in amphid neurons (Brisbin *et al.* 2009) and the specific suppression of *vab-1 (kd)* by *daf-18*, we consider the most likely model that VAB-1 promotes PI3K signaling in amphid axon guidance, either by inhibiting DAF-18 or promoting PI3K activity, or both. Our observations that loss of *daf-18* function both suppresses *vab-1(kd)* and slightly enhances *vab-1(0)* guidance defects may reflect the need for a specific intermediate level of PI3K signaling: partial loss of PI3K signaling, as in *vab-1(kd)* mutants, may be compensated for by reduced DAF-18 activity, whereas in the context of a more complete loss of PI3K signaling as in *vab-1(0)*, the elevated or delocalized PIP2 resulting from lack of DAF-18 function may also affect parallel pathways.

Loss of function in the PI3K target DAF-16/FOXO also suppresses *vab-1* guidance defects. Unexpectedly, loss of function in $PIP_3$-regulated kinases such as AKT-1, SGK-1, or PDK-1 also suppressed *vab-1(kd)* defects. The downstream mechanisms of PI3K signal transduction in axon guidance may therefore differ from those involved in dauer formation or aging.

### *The role of ABL-1 in VAB-1 signaling*

We have shown that the Src family tyrosine kinase ABL-1 promotes amphid axon guidance, likely downstream of VAB-1 signaling. So far, *abl-1* has only been indirectly implicated in *C. elegans* axon guidance (Fox *et al.* 2005); our results provide functional evidence for this role. Interestingly, in mammalian neurons Abl has been shown to mediate EphA-dependent axon repulsion (Harbott and Nobes 2005). The simplest interpretation of our findings in *C. elegans* is that ABL-1 promotes attractive responses to guidance cues. ABL-1 appears to be required in a kinase-independent and EFN-1-independent branch of VAB-1 signaling. ABL-1 might be activated by a nonephrin ligand, or by a ligand-independent activity of VAB-1 as discussed above. In mammalian cells Abl can interact with Eph receptors in multiple ways. In breast cancers, EphB4 can directly interact with Abl, dependent on ligand and kinase activity (Noren *et al.* 2006). Eph receptors can also interact with Abl independent of Eph kinase activity through an interaction mediated by the C-terminal tail of Abl (Yu *et al.* 2001). Although the ABL-1 SH2 domain did not interact with the kinase domain of VAB-1 in two-hybrid assays (Mohamed *et al.* 2012), ABL-1 might interact with VAB-1 indirectly, or via one of the other modes described by Yu *et al.* (2001). Further work will be required to determine the mechanism by which ABL-1 might mediate VAB-1 signals.

Our finding that PI3K and ABL-1 act as parallel outputs in VAB-1-mediated axon guidance (Figure 7A) is interesting in light of the finding that EphB2 signaling in intestinal stem cells also involves parallel PI3K and Abl signals (Genander *et al.* 2009). EphB2 regulates cell positioning in a kinase-independent pathway via PI3K and regulates cell proliferation via a kinase-dependent Abl pathway. Although our

results are more compatible with ABL-1 functioning in a kinase-independent forward signaling pathway, these comparisons suggest Eph signaling operates via a small number of signaling cascades whose outputs are ultimately cell-type specific.

### *Eph signaling has unexpected left–right asymmetry in axon guidance*

It is now well established that amphid neurons display extensive left–right asymmetry in function and in structure. Such asymmetry can be stochastic, as in AWC receptor expression (Troemel *et al.* 1997), or biased, as in ASE receptor expression, sensory function, and axon diameter (Bargmann and Horvitz 1991; Pierce-Shimomura *et al.* 2001; Chang *et al.* 2003; Goldsmith *et al.* 2010). Left–right asymmetry in axon outgrowth has been reported in AIY amphid interneurons (Bertrand *et al.* 2011). Our findings are the first evidence that amphid neurons also display biased asymmetry in their axon guidance.

*vab-1* and *efn* mutants display a consistent and significant left-hand bias in ventral guidance defects. We observed this bias in all amphid neuron classes examined. The inability of the ASEL–ASER left-to-right fate transformation in *lsy-6* mutants to alter this bias is suggestive that the bias reflects an asymmetric signaling environment, although it remains possible that *lsy-6* mutants fail to transform the relevant intrinsic aspects of the ASEL fate. Consistent with this, we find that at least one ephrin, EFN-2, displays highly asymmetric expression in embryonic neurons. Although these studies do not directly address the signaling environment at the time of amphid axon guidance, they are consistent with the idea that axon guidance cues can be highly left–right asymmetric. As *vab-1* null mutants also display asymmetric defects, it appears that other nonephrin cues must also be asymmetric and that this asymmetry is revealed in the absence of VAB-1. However no obvious bias has been reported in the expression or function of the two other main pathways in amphid axon guidance, UNC-6 netrin/UNC-40 and SAX-3/Robo.

Our results also imply a differential reliance on kinase-dependent or kinase-independent signaling on the left and right sides (Figure 7B). As >90% of aberrantly guided axons in *vab-1(kd)* mutants are on the left, the kinase-dependent pathway seems to be most important in left-side guidance. Loss of *efn-2* improves left-hand guidance in *vab-1(kd)* mutants, indicating EFN-2 is inhibitory in this context. This inhibitory effect might reflect the expression of EFN-2 in multiple left-hand amphid neurons, where it could inhibit VAB-1 signaling in *cis* in a manner similar to EFN-1. However in animals lacking EFN-1, loss of EFN-2 exacerbates left-hand guidance defects and improves right-hand defects. In the absence of EFN-1, EFN-2 may play a positive role in left-hand guidance, as it is also asymmetrically expressed in AIYL. EFN-2 does not appear to be expressed in right-hand amphid neurons but could influence guidance from nearby asymmetric sites of expression such as the IL neurons. An interesting possibility is that loss of function in EFN-2 suppresses ventral guidance defects because EFN-2 is involved in promoting guidance to the lateral path. In this model, EFN-2 and EFN-1 act as competing cues for the lateral and ventral paths.

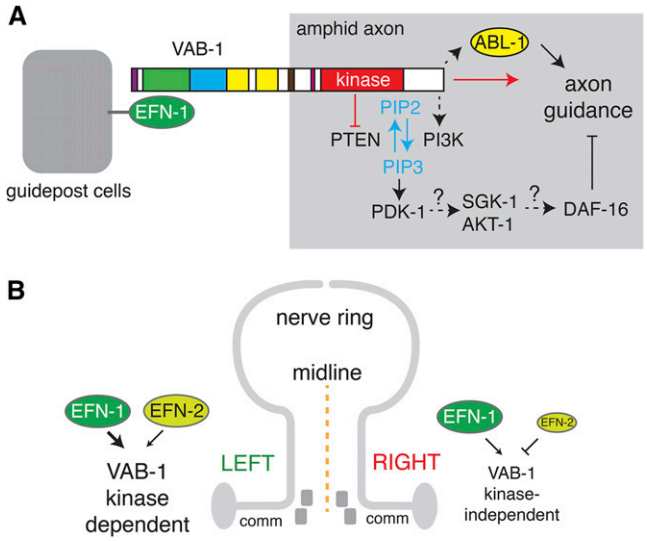


**Figure 7** Models of Eph signaling in amphid axon guidance. (A) Possible relationships between EFN-1, VAB-1, and the PI3K and ABL-1 pathways in axon guidance. (B) Model for the left–right bias in Eph signaling. Amphid guidance on the left side of the animal is mediated by a VAB-1 kinase-dependent signaling pathway. In the presence of EFN-1, EFN-2 inhibits ventral guidance. In the absence of EFN-1, EFN-2 can promote signaling. The right side relies mostly on a kinase-independent signaling mechanism that is inhibited by EFN-2.

### *Axons in the amphid commissure may be guided by pioneer neurons*

A prime question in analyzing guidance of an axon bundle such as the amphid commissure is the extent to which axons are guided independently or by fasciculation with pioneer axons (Lee *et al.* 1997). The all-or-nothing nature of amphid commissure guidance defects has been previously noted (Bülow *et al.* 2002) and suggests amphid axons might follow single pioneer axons. Our analysis extends this picture in that expression of VAB-1 or ABL-1 in a single neuron, AWB, can not only cell autonomously rescue guidance of that neuron, but also may nonautonomously rescue the guidance of other amphid neurons. At present we cannot exclude the possibility that the *str-1* promoter is more widely expressed in amphid neurons early in development; our attempts to use other amphid neuron-specific promoters to rescue amphid guidance were unsuccessful for technical reasons. It is possible that AWB is normally a pioneer axon whose guidance determines the direction of the commissure. Alternatively, VAB-1 or ABL-1 overexpression may sensitize or otherwise give a growth advantage to AWB such that it is able to assume a pioneer function that it does not normally have. An important future goal will be to examine the dynamics of amphid axon outgrowth in these genetic backgrounds.

## Acknowledgments

We thank Max Heiman, Joe Culotti, and Ian Chin-Sang for reagents; Scott Clark, Crystal Lee, and Martin Hudson for new *vab-1* alleles; Asim Alam for characterizing *vab-1* alleles; and Nese Cinar, Jennifer Gotenstein, and Andy Nguyen for help with strain constructions and scoring amphid guidance. Emily Troemel, Elena Pasquale, Zhiping Wang, and Naina Kurup made helpful comments on the manuscript. We thank Sukryool Alan Kang for help with NucleiTracker4D software. Deletion mutations were generated by the *C. elegans* Gene Knockout Consortium and the Japan National Bioresource Project. Some mutations were provided by the Caenorhabditis Genetics Center, which is funded by the National Institutes of Health (NIH) Office of Research Infrastructure Programs (P40 OD010440). E.N.G. was supported by the University of California, San Diego (UCSD)/Salk Training Grant in Developmental Biology of Neural Diseases (T32 HD007495). C.A.G. was supported by the UCSD Neural Circuits Postdoctoral Training Program (T32 NS007220) and by a Ruth S. Kirschstein National Research Service Award (F32 GM090652). This work was supported by an award from the US Public Health Service (NIH R01 GM054657) to A.D.C.

## Literature Cited

Adler, C. E., R. D. Fetter, and C. I. Bargmann, 2006 UNC-6/Netrin induces neuronal asymmetry and defines the site of axon initiation. Nat. Neurosci. 9: 511–518.

Altun-Gultekin, Z., Y. Andachi, E. L. Tsalik, D. Pilgrim, Y. Kohara *et al.*, 2001 A regulatory cascade of three homeobox genes, *ceh-10*, *ttx-3* and *ceh-23*, controls cell fate specification of a defined interneuron class in *C. elegans*. Development 128: 1951–1969.

Bargmann, C. I., and H. R. Horvitz, 1991 Chemosensory neurons with overlapping functions direct chemotaxis to multiple chemicals in *C. elegans*. Neuron 7: 729–742.

Bertrand, V., P. Bisso, R. J. Poole, and O. Hobert, 2011 Notch-dependent induction of left/right asymmetry in *C. elegans* interneurons and motoneurons. Curr. Biol. 21: 1225–1231.

Bonanomi, D., O. Chivatakarn, G. Bai, H. Abdesselem, K. Lettieri *et al.*, 2012 Ret is a multifunctional coreceptor that integrates diffusible- and contact-axon guidance signals. Cell 148: 568–582.

Boulin, T., R. Pocock, and O. Hobert, 2006 A novel Eph receptor-interacting IgSF protein provides *C. elegans* motoneurons with midline guidepost function. Curr. Biol. 16: 1871–1883.

Brisbin, S., J. Liu, J. Boudreau, J. Peng, M. Evangelista *et al.*, 2009 A role for *C. elegans* Eph RTK signaling in PTEN regulation. Dev. Cell 17: 459–469.

Bruckner, K., J. Pablo Labrador, P. Scheiffele, A. Herb, P. H. Seeburg *et al.*, 1999 EphrinB ligands recruit GRIP family PDZ adaptor proteins into raft membrane microdomains. Neuron 22: 511–524.

Bülow, H. E., K. L. Berry, L. H. Topper, E. Peles, and O. Hobert, 2002 Heparan sulfate proteoglycan-dependent induction of axon branching and axon misrouting by the Kallmann syndrome gene *kal-1*. Proc. Natl. Acad. Sci. USA 99: 6346–6351.

Carvalho, R. F., M. Beutler, K. J. Marler, B. Knoll, E. Becker-Barroso *et al.*, 2006 Silencing of EphA3 through a cis interaction with ephrinA5. Nat. Neurosci. 9: 322–330.

Catchpole, T., and M. Henkemeyer, 2011 EphB2 tyrosine kinase-dependent forward signaling in migration of neuronal progenitors that populate and form a distinct region of the dentate niche. J. Neurosci. 31: 11472–11483.

Chan, S. S., H. Zheng, M. W. Su, R. Wilk, M. T. Killeen *et al.*, 1996 UNC-40, a *C. elegans* homolog of DCC (Deleted in Colorectal Cancer), is required in motile cells responding to UNC-6 netrin cues. Cell 87: 187–195.

Chang, C., C. E. Adler, M. Krause, S. G. Clark, F. B. Gertler *et al.*, 2006 MIG-10/lamellipodin and AGE-1/PI3K promote axon guidance and outgrowth in response to slit and netrin. Curr. Biol. 16: 854–862.

Chang, S., R. J. Johnston, Jr., and O. Hobert, 2003 A transcriptional regulatory cascade that controls left/right asymmetry in chemosensory neurons of *C. elegans*. Genes Dev. 17: 2123–2137.

Cheng, H., J. A. Govindan, and D. Greenstein, 2008 Regulated trafficking of the MSP/Eph receptor during oocyte meiotic maturation in *C. elegans*. Curr. Biol. 18: 705–714.

Chin-Sang, I. D., S. E. George, M. Ding, S. L. Moseley, A. S. Lynch *et al.*, 1999 The ephrin VAB-2/EFN-1 functions in neuronal signaling to regulate epidermal morphogenesis in *C. elegans*. Cell 99: 781–790.

Chin-Sang, I. D., S. L. Moseley, M. Ding, R. J. Harrington, S. E. George *et al.*, 2002 The divergent *C. elegans* ephrin EFN-4 functions inembryonic morphogenesis in a pathway independent of the VAB-1 Eph receptor. Development 129: 5499–5510.

Christensen, R., L. de la Torre-Ubieta, A. Bonni, and D. A. Colon-Ramos, 2011 A conserved PTEN/FOXO pathway regulates neuronal morphology during *C. elegans* development. Development 138: 5257–5267.

Cowan, C. A., N. Yokoyama, L. M. Bianchi, M. Henkemeyer, and B. Fritzsch, 2000 EphB2 guides axons at the midline and is necessary for normal vestibular function. Neuron 26: 417–430.

Davy, A., N. W. Gale, E. W. Murray, R. A. Klinghoffer, P. Soriano *et al.*, 1999 Compartmentalized signaling by GPI-anchored ephrin-A5 requires the Fyn tyrosine kinase to regulate cellular adhesion. Genes Dev. 13: 3125–3135.

Drescher, U., C. Kremoser, C. Handwerker, J. Loschinger, M. Noda *et al.*, 1995 In vitro guidance of retinal ganglion cell axons by RAGS, a 25 kDa tectal protein related to ligands for Eph receptor tyrosine kinases. Cell 82: 359–370.

Egea, J., and R. Klein, 2007 Bidirectional Eph-ephrin signaling during axon guidance. Trends Cell Biol. 17: 230–238.

Finney, M., and G. Ruvkun, 1990 The unc-86 gene product couples cell lineage and cell identity in C. elegans. Cell 63: 895–905.

Fox, R. M., S. E. Von Stetina, S. J. Barlow, C. Shaffer, K. L. Olszewski *et al.*, 2005 A gene expression fingerprint of *C. elegans* embryonic motor neurons. BMC Genomics 6: 42.

Frøkjaer-Jensen, C., K. S. Kindt, R. A. Kerr, H. Suzuki, K. Melnik-Martinez *et al.*, 2006 Effects of voltage-gated calcium channel subunit genes on calcium influx in cultured *C. elegans* mechanosensory neurons. J. Neurobiol. 66: 1125–1139.

Genander, M., M. M. Halford, N. J. Xu, M. Eriksson, Z. Yu *et al.*, 2009 Dissociation of EphB2 signaling pathways mediating progenitor cell proliferation and tumor suppression. Cell 139: 679–692.

George, S. E., K. Simokat, J. Hardin, and A. D. Chisholm, 1998 The VAB-1 Eph receptor tyrosine kinase functions in neural and epithelial morphogenesis in *C. elegans*. Cell 92: 633–643.

Giurumescu, C. A., S. Kang, T. A. Planchon, E. Betzig, J. Bloomekatz *et al.*, 2012 Quantitative semi-automated analysis of morphogenesis with single-cell resolution in complex embryos. Development 139: 4271–4279.

Goldsmith, A. D., S. Sarin, S. Lockery, and O. Hobert, 2010 Developmental control of lateralized neuron size in the nematode *Caenorhabditis elegans*. Neural Dev. 5: 33.

Gu, C., and S. Park, 2001 The EphA8 receptor regulates integrin activity through p110ϒ phosphatidylinositol-3 kinase in a tyrosine kinase activity-independent manner. Mol. Cell. Biol. 21: 4579–4597.

Gu, C., and S. Park, 2003 The p110 gamma PI-3 kinase is required for EphA8-stimulated cell migration. FEBS Lett. 540: 65–70.

Hansen, M. J., G. E. Dallal, and J. G. Flanagan, 2004 Retinal axon response to ephrin-as shows a graded, concentration-dependent transition from growth promotion to inhibition. Neuron 42: 717–730.

Harbott, L. K., and C. D. Nobes, 2005 A key role for Abl family kinases in EphA receptor-mediated growth cone collapse. Mol. Cell. Neurosci. 30: 1–11.

Hedgecock, E. M., J. G. Culotti, J. N. Thomson, and L. A. Perkins, 1985 Axonal guidance mutants of *Caenorhabditis elegans* identified by filling sensory neurons with fluorescein dyes. Dev. Biol. 111: 158–170.

Heiman, M. G., and S. Shaham, 2009 DEX-1 and DYF-7 establish sensory dendrite length by anchoring dendritic tips during cell migration. Cell 137: 344–355.

Hertweck, M., C. Gobel, and R. Baumeister, 2004 *C. elegans* SGK-1 is the critical component in the Akt/PKB kinase complex to control stress response and life span. Dev. Cell 6: 577–588.

Hindges, R., T. McLaughlin, N. Genoud, M. Henkemeyer, and D. D. O'Leary, 2002 EphB forward signaling controls directional branch extension and arborization required for dorsal-ventral retinotopic mapping. Neuron 35: 475–487.

Hobert, O., I. Mori, Y. Yamashita, H. Honda, Y. Ohshima *et al.*, 1997 Regulation of interneuron function in the *C. elegans* thermoregulatory pathway by the *ttx-3* LIM homeobox gene. Neuron 19: 345–357.

Hobert, O., R. J. Johnston, Jr., and S. Chang, 2002 Left-right asymmetry in the nervous system: the *Caenorhabditis elegans* model. Nat. Rev. Neurosci. 3: 629–640.

Ikegami, R., H. Zheng, S. H. Ong, and J. Culotti, 2004 Integration of semaphorin-2A/MAB-20, ephrin-4, and UNC-129 TGF-beta signaling pathways regulates sorting of distinct sensory rays in *C. elegans*. Dev. Cell 6: 383–395.

Ikegami, R., K. Simokat, H. Zheng, L. Brown, G. Garriga *et al.*, 2012 Semaphorin and Eph receptor signaling guide a series of cell movements for ventral enclosure in *C. elegans*. Curr. Biol. 22: 1–11.

Johnston, R. J., and O. Hobert, 2003 A microRNA controlling left/right neuronal asymmetry in *Caenorhabditis elegans*. Nature 426: 845–849.

Knoll, B., and U. Drescher, 2004 Src family kinases are involved in EphA receptor-mediated retinal axon guidance. J. Neurosci. 24: 6248–6257.

Kullander, K., and R. Klein, 2002 Mechanisms and functions of Eph and ephrin signalling. Nat. Rev. Mol. Cell Biol. 3: 475–486.

Labouesse, M., S. Sookhareea, and H. R. Horvitz, 1994 The *Caenorhabditis elegans* gene *lin-26* is required to specify the fates of hypodermal cells and encodes a presumptive zinc-finger transcription factor. Development 120: 2359–2368.

Lee, R. Y., L. Lobel, M. Hengartner, H. R. Horvitz, and L. Avery, 1997 Mutations in the alpha1 subunit of an L-type voltage-activated Ca2+ channel cause myotonia in *Caenorhabditis elegans*. EMBO J. 16: 6066–6076.

Lim, Y. S., T. McLaughlin, T. C. Sung, A. Santiago, K. F. Lee *et al.*, 2008 p75(NTR) mediates ephrin-A reverse signaling required for axon repulsion and mapping. Neuron 59: 746–758.

Lin, K., J. B. Dorman, A. Rodan, and C. Kenyon, 1997 *daf-16*: an HNF-3/forkhead family member that can function to double the life-span of *Caenorhabditis elegans*. Science 278: 1319–1322.

Maduro, M., and D. Pilgrim, 1995 Identification and cloning of *unc-119*, a gene expressed in the *Caenorhabditis elegans* nervous system. Genetics 141: 977–988.

Manning, G., 2005 Genomic overview of protein kinases (December 13, 2005), WormBook, ed. The *C. elegans* Research Community, WormBook, doi/10.1895/wormbook.1.60.1, http://www.wormbook.org.

Marler, K. J., E. Becker-Barroso, A. Martinez, M. Llovera, C. Wentzel *et al.*, 2008 A TrkB/EphrinA interaction controls retinal axon branching and synaptogenesis. J. Neurosci. 28: 12700–12712.

Miller, M. A., and I. D. Chin-Sang, 2012 Eph receptor signaling in *C. elegans* (November 29, 2012), WormBook, ed. The *C. elegans* Research Community, WormBook, doi/10.1895/wormbook.1.151.1, http://www.wormbook.org.

Miller, M. A., P. J. Ruest, M. Kosinski, S. K. Hanks, and D. Greenstein, 2003 An Eph receptor sperm-sensing control mechanism for oocyte meiotic maturation in *Caenorhabditis elegans*. Genes Dev. 17: 187–200.

Mohamed, A. M., and I. D. Chin-Sang, 2006 Characterization of loss-of-function and gain-of-function Eph receptor tyrosine kinase signaling in *C. elegans* axon targeting and cell migration. Dev. Biol. 290: 164–176.

Mohamed, A. M., J. R. Boudreau, F. P. Yu, J. Liu, and I. D. Chin-Sang, 2012 The *Caenorhabditis elegans* Eph receptor activates NCK and N-WASP, and inhibits Ena/VASP to regulate growth cone dynamics during axon guidance. PLoS Genet. 8: e1002513.

Noren, N. K., and E. B. Pasquale, 2004 Eph receptor-ephrin bidirectional signals that target Ras and Rho proteins. Cell. Signal. 16: 655–666.

Noren, N. K., G. Foos, C. A. Hauser, and E. B. Pasquale, 2006 The EphB4 receptor suppresses breast cancer cell tumorigenicity through an Abl-Crk pathway. Nat. Cell Biol. 8: 815–825.

Noren, N. K., N. Y. Yang, M. Silldorff, R. Mutyala, and E. B. Pasquale, 2009 Ephrin-independent regulation of cell substrate adhesion by the EphB4 receptor. Biochem. J. 422: 433–442.

Ogg, S., and G. Ruvkun, 1998 The *C. elegans* PTEN homolog, DAF-18, acts in the insulin receptor-like metabolic signaling pathway. Mol. Cell 2: 887–893.

Ogg, S., S. Paradis, S. Gottlieb, G. I. Patterson, L. Lee *et al.*, 1997 The Fork head transcription factor DAF-16 transduces insulin-like metabolic and longevity signals in *C. elegans*. Nature 389: 994–999.

Pandey, A., D. F. Lazar, A. R. Saltiel, and V. M. Dixit, 1994 Activation of the Eck receptor protein tyrosine kinase stimulates phosphatidylinositol 3-kinase activity. J. Biol. Chem. 269: 30154–30157.

Paradis, S., and G. Ruvkun, 1998 *Caenorhabditis elegans* Akt/PKB transduces insulin receptor-like signals from AGE-1 PI3 kinase to the DAF-16 transcription factor. Genes Dev. 12: 2488–2498.

Paradis, S., M. Ailion, A. Toker, J. H. Thomas, and G. Ruvkun, 1999 A PDK1 homolog is necessary and sufficient to transduce AGE-1 PI3 kinase signals that regulate diapause in *Caenorhabditis elegans*. Genes Dev. 13: 1438–1452.

Pasquale, E. B., 2005 Eph receptor signalling casts a wide net on cell behaviour. Nat. Rev. Mol. Cell Biol. 6: 462–475.

Pasquale, E. B., 2008 Eph-ephrin bidirectional signaling in physiology and disease. Cell 133: 38–52.

Pierce-Shimomura, J. T., S. Faumont, M. R. Gaston, B. J. Pearson, and S. R. Lockery, 2001 The homeobox gene *lim-6* is required for distinct chemosensory representations in *C. elegans*. Nature 410: 694–698.

Sahin, M., P. L. Greer, M. Z. Lin, H. Poucher, J. Eberhart *et al.*, 2005 Eph-dependent tyrosine phosphorylation of ephexin1 modulates growth cone collapse. Neuron 46: 191–204.

Satterlee, J. S., H. Sasakura, A. Kuhara, M. Berkeley, I. Mori *et al.*, 2001 Specification of thermosensory neuron fate in *C. elegans* requires *ttx-1*, a homolog of otd/Otx. Neuron 31: 943–956.

Shamah, S. M., M. Z. Lin, J. L. Goldberg, S. Estrach, M. Sahin *et al.*, 2001 EphA receptors regulate growth cone dynamics through

the novel guanine nucleotide exchange factor ephexin. Cell 105: 233–244.

Shin, J., C. Gu, E. Park, and S. Park, 2007 Identification of phosphotyrosine binding domain-containing proteins as novel downstream targets of the EphA8 signaling function. Mol. Cell. Biol. 27: 8113–8126.

Smith, A., V. Robinson, K. Patel, and D. G. Wilkinson, 1997 The EphA4 and EphB1 receptor tyrosine kinases and ephrin-B2 ligand regulate targeted migration of branchial neural crest cells. Curr. Biol. 7: 561–570.

Sulston, J. E., E. Schierenberg, J. G. White, and J. N. Thomson, 1983 The embryonic cell lineage of the nematode *Caenorhabditis elegans*. Dev. Biol. 100: 64–119.

Troemel, E. R., B. E. Kimmel, and C. I. Bargmann, 1997 Reprogramming chemotaxis responses: sensory neurons define olfactory preferences in *C. elegans*. Cell 91: 161–169.

Wahl, S., H. Barth, T. Ciossek, K. Aktories, and B. K. Mueller, 2000 Ephrin-A5 induces collapse of growth cones by activating Rho and Rho kinase. J. Cell Biol. 149: 263–270.

Wang, X., P. J. Roy, S. J. Holland, L. W. Zhang, J. G. Culotti *et al.*, 1999 Multiple ephrins control cell organization in *C. elegans* using kinase-dependent and -independent functions of the VAB-1 Eph receptor. Mol. Cell 4: 903–913.

Yokoyama, N., M. I. Romero, C. A. Cowan, P. Galvan, F. Helmbacher *et al.*, 2001 Forward signaling mediated by ephrin-B3 prevents contralateral corticospinal axons from recrossing the spinal cord midline. Neuron 29: 85–97.

Yoshimura, S., J. I. Murray, Y. Lu, R. H. Waterston, and S. Shaham, 2008 *mls-2* and *vab-3* control glia development, *hlh-17*/Olig expression and glia-dependent neurite extension in *C. elegans*. Development 135: 2263–2275.

Yu, H. H., A. H. Zisch, V. C. Dodelet, and E. B. Pasquale, 2001 Multiple signaling interactions of Abl and Arg kinases with the EphB2 receptor. Oncogene 20: 3995–4006.

Zallen, J. A., B. A. Yi, and C. I. Bargmann, 1998 The conserved immunoglobulin superfamily member SAX-3/Robo directs multiple aspects of axon guidance in *C. elegans*. Cell 92: 217–227.

Zallen, J. A., S. A. Kirch, and C. I. Bargmann, 1999 Genes required for axon pathfinding and extension in the *C. elegans* nerve ring. Development 126: 3679–3692.

Zisch, A. H., M. S. Kalo, L. D. Chong, and E. B. Pasquale, 1998 Complex formation between EphB2 and Src requires phosphorylation of tyrosine 611 in the EphB2 juxtamembrane region. Oncogene 16: 2657–2670.

*Communicating editor: M. Sundaram*

GENETICS

**Supporting Information**
http://www.genetics.org/lookup/suppl/doi:10.1534/genetics.113.154393/-/DC1

# Mechanisms of Ephrin Receptor Protein Kinase-Independent Signaling in Amphid Axon Guidance in *Caenorhabditis elegans*

**Emily N. Grossman, Claudiu A. Giurumescu, and Andrew D. Chisholm**


DOI: 10.1534/genetics.113.154393

**Table S1 Transgenic *C. elegans* strains and plasmids**

| Transgene | DNA constructs | Genotype | Strain # |
|---|---|---|---|
| *juEx16** | VAB-1(+) cosmid (M03A1) | *vab-1(0); kyIs104* | CZ11816 |
| *juEx2870* | VAB-1(+) fosmid (WRM0617bA10) (100ng/µl) | *vab-1(0); kyIs104* | CZ14390 |
| *juEx3839* | VAB-1(+) minigene (pCZ55) (1ng/µl) | *vab-1(0); kyIs104* | CZ14800 |
| *juEx3529* | P*unc-33*-VAB-1 (*vab-1* 3'UTR) (pCZGY1859) (1ng/µl) | *vab-1(0); kyIs104* | CZ14078 |
| *juEx3470* | P*rgef-1*-VAB-1 (*vab-1* 3'UTR) (pCZGY1847) (1 ng/µl) | *vab-1(0); kyIs104* | CZ14082 |
| *juEx3836* | P*myo-2*-VAB-1 (*vab-1* 3'UTR) (pCZGY1854) (1 ng/µl) | *vab-1(0); kyIs104* | CZ14713 |
| *juEx4725* | P*lin-26*-VAB-1 (*vab-1* 3'UTR) (pCZGY2220) (1 ng/µl) | *vab-1(0); kyIs104* | CZ16392 |
| *juEx4728* | P*hlh-17*-VAB-1 (*vab-1* 3'UTR) (pCZGY1852) (1 ng/µl) | *vab-1(0); kyIs104* | CZ16835 |
| *juEx3308* | P*dyf-7*-VAB-1 (*vab-1* 3'UTR) (pCZGY1342) (15 ng/µl) | *vab-1(0); kyIs104* | CZ13960 |
| *juEx4527* | P*ttx-3*-VAB-1 (*vab-1* 3'UTR) (pCZGY1841) (5 ng/µl) | *vab-1(0); kyIs104* | CZ16033 |
| *juEx4857* | P*str-1*-VAB-1 (*vab-1* 3'UTR) (pCZGY2221) (1 ng/µl) | *vab-1(0); kyIs104* | CZ17039 |
| *juEx3179* | P*dyf-7*-EFN-1 (*unc-54* 3'UTR) (pCZGY1340) (1 ng/µl) | *vab-1(0); kyIs104* | CZ17654 |
| *juEx5418* | P*dyf-7*-EFN-2 (*unc-54* 3'UTR) (pCZGY1343) (1 ng/µl) | *vab-1(0); kyIs104* | CZ18326 |
| *juEx127*** | EFN-1(+) (pCZ126) (50 ng/µl) | *efn-1(0); kyIs104* | CZ14447 |
| *juIs52*** | EFN-1::GFP (pCZ131) (50 ng/µl) | *efn-1(0); kyIs104* | CZ13080 |
| *juEx3775* | P*dpy-30*-EFN-1 (*unc-54* 3'UTR) (pCZGY1843) (1 ng/µl) | *efn-1(0); kyIs104* | CZ14487 |
| *juEx3577* | P*unc-33*-EFN-1 (*efn-1* 3'UTR) (pCZGY1857) (1 ng/µl) | *efn-1(0); kyIs104* | n/a |
| *juEx3476* | P*unc-119*-EFN-1 (*unc-54* 3'UTR) (pCZGY1860) (1 ng/µl) | *efn-1(0); kyIs104* | CZ14086 |
| *juEx3158* | P*rgef-1*-EFN-1 (*unc-54* 3'UTR) (pCZGY1344) (1 ng/µl) | *efn-1(0); kyIs104* | CZ13372 |
| *juEx3835* | P*myo-2*-EFN-1 (*efn-1* 3'UTR) (pCZGY1853) (1 ng/µl) | *efn-1(0); kyIs104* | CZ14694 |
| *juEx4864* | P*hlh-17*-EFN-1 (*efn-1* 3'UTR) (pCZGY1851) (1 ng/µl) | *efn-1(0); kyIs104* | CZ17042 |
| *juEx4524* | P*ttx-3*-EFN-1 (*efn-1* 3'UTR) (pCZGY1839) (5 ng/µl) | *efn-1(0); kyIs104* | CZ16028 |
| *juEx4860* | P*lin-26*-EFN-1 (*efn-1* 3'UTR) (pCZGY2223) (1 ng/µl) | *efn-1(0); kyIs104* | CZ16642 |
| *juEx3179* | P*dyf-7*-EFN-1 (*unc-54* 3'UTR) (pCZGY1340) (1 ng/µl) | *efn-1(0); kyIs104* | CZ13373 |
| *juEx3272* | P*dyf-7*-EFN-1 (*efn-1* 3'UTR) (pCZGY1341) (1 ng/µl) | *efn-1(0); kyIs104* | CZ13965 |

| | | | |
|---|---|---|---|
| *juEx4909* | P*str-1*-EFN-1 (*efn-1* 3'UTR) (pCZGY2224) (1 ng/µl) | *efn-1(0); kyIs104* | CZ16743 |
| *juEx4344* | P*dyf-7*-ABL-1 (*abl-1* 3'UTR) (pCZGY1845) (1 ng/µl) | *vab-1(kd); abl-1; kyIs104* | CZ15789 |
| *juEx4345* | P*dyf-7*-ABL-1 (*abl-1* 3'UTR) (pCZGY1845) (1 ng/µl) | *vab-1(kd); abl-1; kyIs104* | CZ15791 |
| *juEx4345* | P*dyf-7*-ABL-1 (*abl-1* 3'UTR) (pCZGY1845) (1 ng/µl) | *vab-1(0); kyIs104* | CZ18522 |
| *juEx5055* | P*str-1*-ABL-1 (*abl-1* 3'UTR) (pCZGY2227) (25 ng/µl) | *vab-1(kd); abl-1; kyIs104* | CZ17047 |
| *juEx5057* | P*str-1*-ABL-1 (*abl-1* 3'UTR) (pCZGY2227) (25 ng/µl) | *vab-1(kd); abl-1; kyIs104* | CZ17049 |
| *juEx5059* | P*str-1*-ABL-1 (*abl-1* 3'UTR) (pCZGY2227) (25 ng/µl) | *vab-1(kd); abl-1; kyIs104* | CZ17051 |
| *juEx5059* | P*str-1*-ABL-1 (*abl-1* 3'UTR) (pCZGY2227) (25 ng/µl) | *vab-1(kd); kyIs104* | CZ18664 |

* GEORGE ET AL., 1998.

** CHIN-SANG ET AL., 1999.

**Table S2 Cells expressing P*efn-2*-mCherry at 335 minutes post fertilization**

| Symmetrical pairs | Right side only | Left side only |
|---|---|---|
| SIAVL(ABplpapappa) | RIS(ABprpappapa) | **AWAL(ABplaapapaa)** |
| SIAVR(ABprpapappa) | IL2R(ABalaappppp) | **ASJL/AUAL(ABalpppppppp)** |
| AVKL(ABplpapapap) | IL1VR/X(ABarappppa) | **AIYL(ABplpapaaap)** |
| AVKR(ABprpapapap) | IL2VR(ABarappppp) | **ASEL/X(ABalpppppppa)** |
| exc gl L(ABplpapapaa) | X/SMBDR(ABarappapap) | **ASKL/X(ABalpppappp)** |
| exc gl R(ABprpapapaa) | DB4(ABprpappapp) | **ASGL(ABplaapapap)** |
| SMBVL(ABalpapappp) | G1(ABprpaaaapa) | **AWBL(ABalpppppap)** |
| SMBVR(ABarappappp) | m6VR(MSpapappa) | RIGL(ABplppappaa) |
| AIBL(ABplaapappa) | m5VR(MSpapaaap) | ADFL(ABalpppppaa) |
| AIBR(ABpraapappa) | RIR(ABprpappppaa) | X/SMBDL(ABalpapapap) |
| ASIL/X(ABplaapappp) | DA8(ABprpapappp) | DD3(ABplppappppa) |
| ASIR/X(ABpraapappp) | DB2(ABarappappa) | DA6(ABplpppaaap) |
| RIML(ABplppaapap) | DB7(ABprppaappp) | arc ant V(ABalpapaapa) |
| RIMR(ABprppaapap) | AVG(ABprpappppap) | hyp2V(ABalpapaaap) |
| AIAL(ABplppaappa) | OLLR/X(ABpraaapapa) | SMDDL(ABplpapaaaa) |
| AIAR(ABprppaappa) | | DB5(ABplpapappp) |
| RMDDL(ABalpapapaa) | | DD1(ABplppappap) |
| RMDDR(ABarappapaa) | | DB6(ABplppaappp) |
| | | M(MSapaapp) |
| | | mu bod(MSappapp) |

P*efn*-2-mCherry expression is overall in more left-hand members of bilaterally symmetric pairs than in right-hand members, including several amphid sensory neurons and amphid interneurons, or their parents (**bold**). A full list of *efn-2*-expressing cells from 305 to 345 minutes of development is available on request.